Inorganic Chemistry

pubs.acs.org/IC

Article

Diphosphine Bioconjugates via Pt(0)-Catalyzed Hydrophosphination. A Versatile Chelator Platform for Technetium-99m and Rhenium-188 Radiolabeling of Biomolecules

Rachel E. Nuttall, Truc Thuy Pham, Ailis C. Chadwick, Ingebjørg N. Hungnes, George Firth, Martin A. Heckenast, Hazel A. Sparkes, M. Carmen Galan,* Michelle T. Ma,* and Paul G. Pringle*

Cite This: https://doi.org/10.1021/acs.inorgchem.2c04008

Read Online

ACCESS | Metrics & More | Article Recommendations | Supporting Information

ABSTRACT: The ability to append targeting biomolecules to chelators that efficiently coordinate to the diagnostic imaging radionuclide, ^{99m}Tc, and the therapeutic radionuclide, ^{188}Re, can potentially enable receptor-targeted "theranostic" treatment of disease. Here we show that Pt(0)-catalyzed hydrophosphination reactions are well-suited to the derivatization of diphosphines with biomolecular moieties enabling the efficient synthesis of ligands of the type $Ph_2PCH_2CH_2P(CH_2CH_2{-}Glc)_2$ (**L**, where Glc = a glucose moiety) using the readily accessible $Ph_2PCH_2CH_2PH_2$ and acryl derivatives. It is shown that hydrophosphination of an acrylate derivative of a deprotected glucose can be carried out in aqueous media. Furthermore, the resulting glucose−chelator conjugates can be radiolabeled with either ^{99m}Tc(V) or ^{188}Re(V) in high radiochemical yields (>95%), to furnish separable mixtures of *cis*- and *trans*-$[M(O)_2L_2]^+$ (M = Tc, Re). Single photon emission computed tomography (SPECT) imaging and *ex vivo* biodistribution in healthy mice show that each isomer possesses favorable pharmacokinetic properties, with rapid clearance from blood circulation via a renal pathway. Both *cis*-$[^{99m}Tc(O)_2L_2]^+$ and *trans*-$[^{99m}Tc(O)_2L_2]^+$ exhibit high stability in serum. This new class of functionalized diphosphine chelators has the potential to provide access to receptor-targeted dual diagnostic/therapeutic pairs of radiopharmaceutical agents, for molecular ^{99m}Tc SPECT imaging and ^{188}Re systemic radiotherapy.

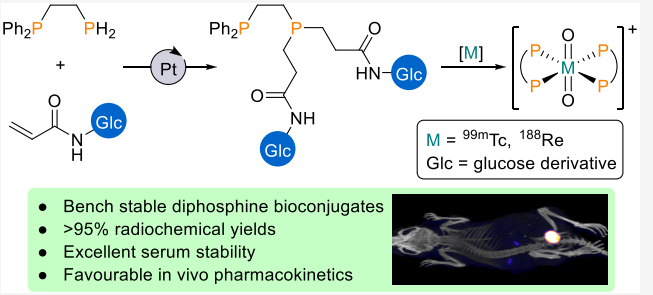

INTRODUCTION

The radioactive, γ-emitting isotope, technetium-99m (^{99m}Tc, $t_{1/2}$ = 6 h, 90% γ, 140 keV), is widely and routinely used in radiotracers for clinical diagnostic SPECT (Single Photon Emission Computed Tomography) or γ-scintigraphy imaging of disease. Currently, ^{99m}Tc imaging uses radiotracers that measure perfusion physiological processes. These ^{99m}Tc-labeled radiopharmaceuticals are based on relatively simple, low molecular weight Tc complexes, and their physicochemical properties determine the biodistribution and disease-targeting capabilities.[1] By contrast, radiopharmaceuticals that have more recently entered routine clinical use target receptors that are overexpressed in diseased tissue. These radiopharmaceuticals include PET (Positron Emission Tomography) diagnostic imaging agents, as well as therapeutic systemic agents that emit cytotoxic β^- or α particles. Pairs of diagnostic imaging and therapeutic radiotracers that target the same receptor are often considered "companion" or "theranostic" agents. Many of these compounds are based on radiometallic ions that are coordinated by a chelator, which in turn is attached to a biomolecule that targets receptors of diseased tissue (Scheme 1).[2] For example, paired ^{68}Ga-labeled peptides for diagnostic PET imaging and ^{177}Lu-labeled peptides for systemic

Scheme 1. General Strategy for Targeted Radiopharmaceuticals, with Amide Coupling Exemplifying a Method of Bioconjugation

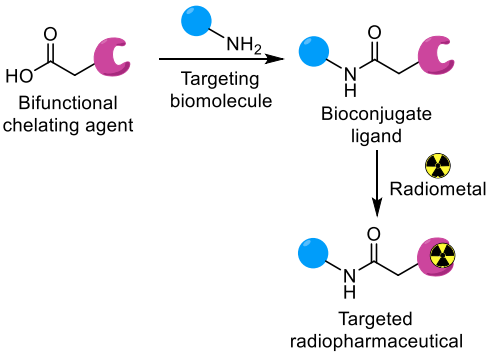

Special Issue: Inorganic Chemistry of Radiopharmaceuticals

Received: November 14, 2022

therapeutic agents have improved treatment outcomes for neuroendocrine and prostate cancer patients.[3−5] New chelator platforms that enable attachment of a chelator to a biomolecule, and form stable complexes of ^{99m}Tc, have potential utility for developing novel ^{99m}Tc radiopharmaceuticals for use in receptor-targeted SPECT/γ-scintigraphy imaging of disease.

The chemistry of Re and Tc are closely similar, and, as Tc has no stable isotopes, the isostructural, naturally occurring rhenium (^{nat}Re) compounds are often used to aid chemical characterization of new ^{99m}Tc-labeled tracers.[6] Significantly, there are two β^--emitting radioisotopes of Re that have suitable decay properties for systemic radiotherapy: ^{186}Re (β^-, 1.07 MeV, 92.5%; γ, 137 and 123 keV, 7.5%; $t_{1/2}$ = 90 h) and ^{188}Re (β^-, 2.1 MeV, 71%; γ, 155 keV, 15%; $t_{1/2}$ = 17 h). Pairs of isostructural ^{99m}Tc and $^{186/188}$Re complexes have potential applications as dual diagnostic/therapeutic radiopharmaceuticals.[7] Additionally, both ^{99m}Tc and ^{188}Re are available from benchtop generators, allowing economically viable and reliable access to these isotopes—essential criteria for many clinical applications.

Diphosphine chelators have actual and potential utility in ^{99m}Tc and ^{188}Re radiopharmaceuticals. The radiopharmaceutical [^{99m}Tc(O)$_2$(tetrofosmin)$_2$]$^+$, known as *Myoview*, is used routinely for imaging cardiac perfusion; it is a ^{99m}Tc(V) complex containing two **tetrofosmin** chelates (Chart 1).[8]

Chart 1. Literature Examples of Phosphine-Containing Chelators for [M(O)$_2$]$^+$ core (M = ^{99m}Tc or ^{188}Re)[8−11]

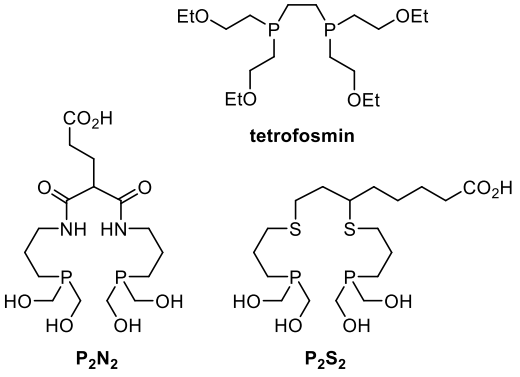

Tetradentate $\mathbf{P_2N_2}$ and $\mathbf{P_2S_2}$ ligands (Chart 1) have also previously been synthesized and radiolabeled with [^{99m}Tc(O)$_2$]$^+$ and [^{188}Re(O)$_2$]$^+$ cores in high radiochemical yield, using simple radiosynthetic protocols suitable for clinical application.[9−11] In addition, the $\mathbf{P_2N_2}$ and $\mathbf{P_2S_2}$ ligands have been conjugated with peptides via amidation of the carboxylic acid groups.[9−11]

Orthogonal azide−alkyne chemistry is frequently employed to attach chelators to biological vectors that target receptors of diseased tissue.[12−15] However, this "click" approach is problematic for tertiary phosphines since they generally react rapidly with azides to form iminophosphines, R′N=PR$_3$ (i.e., the Staudinger Reaction) which eliminates the P-binding function. The two following strategies have been previously employed to circumvent this Staudinger problem for click chemistry with phosphines (designed for applications as ligands in homogeneous catalysis), but neither is appropriate for bioconjugation. (1) The phosphine is introduced into an existing triazole group, but reactive chlorophosphine and organolithium reagents are required,[16] which are incompatible with the presence of many O- and N- functional groups without extensive protection/deprotection protocols. (2) The phosphine is protected by peroxide oxidation to O=PR$_3$ prior to undertaking a click reaction, and then after the click reaction is completed, hydridic reduction is carried out to regenerate the PR$_3$ donor,[17] but again, these manipulations involve reagents that are generally incompatible with functional groups in biomolecules.

The addition of a H−P^{III} bond to an unsaturated C−C bond (hydrophosphination) is an atom-efficient, versatile, and generally irreversible way of making phosphine ligands.[18−29] Platinum(0)-catalyzed hydrophosphination is a reliable route to phosphines that contain reactive functional groups suitable for further elaboration.[30−36] We have recently demonstrated that the air-stable diphosphine Ph$_2$PCH$_2$CH$_2$PR$_2$ (where R = CH$_2$CH$_2$CO$_2$Me) (**L1**) is readily prepared from Ph$_2$PCH$_2$CH$_2$PH$_2$ and methyl acrylate via the Pt(0)-catalyzed hydrophosphination reaction shown in Scheme 2.[30] Many

Scheme 2. Synthesis of Functionalized Diphosphines via Pt(0)-Catalyzed Hydrophosphination of CH$_2$=CHZ, (Z = CO$_2$R, CONR$_2$, CN) by a Tertiary-Primary Diphosphine[a]

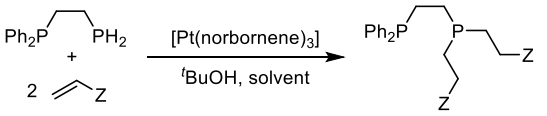

[a]The protic additive *t*-BuOH inhibits the formation of telomeric byproducts.[37]

acryl derivatives are readily accessible synthetically, potentially paving the way for hydrophosphination to provide a simple route to diphosphines with appended biologically targeting motifs.

Carbohydrates and their glycoconjugates mediate a wide range of biological processes and therefore can provide highly specific glycan markers of diseased cells that can be exploited for early diagnosis and in drug development. Although carbohydrates are the most diverse and one of the most important classes of biomolecules in nature, there are relatively few carbohydrate-based drugs in clinical use.[38] Glucose derivatives have been widely used to target glucose-avid diseased tissue, such as cancer, or to improve the solubility, biological stability, or other pharmacological properties of drugs.[39] The radioactive ^{18}F-labeled glucose derivative, [^{18}F]-FDG ([^{18}F]-2-fluoro-2-deoxyglucose), is taken up by the GLUT1 transporter which is overexpressed in cancer, and [^{18}F]-FDG is routinely used as a diagnostic PET imaging agent in oncology.[40,41] We have selected glucose derivatives as model biomolecules to assess the feasibility of bioconjugation using Pt(0)-catalyzed hydrophosphination. One attraction of glucose as the target motif is that it can be derivatized from either hydroxy-protected or unprotected precursors, allowing the versatility and scope of Pt(0)-catalyzed hydrophosphination to be gauged. Furthermore, the resulting phosphine-glucose bioconjugates are likely to be highly hydrophilic, allowing the stability of the bioconjugates and their complexes in aqueous solutions and biological media to be assessed.

Herein we report the application of Pt(0)-catalyzed hydrophosphination (Scheme 2),[30] in the production of diphosphine glycoconjugates with potential utility as Tc/Re radiotheranostics. It is shown that diphosphine derivatives of

https://doi.org/10.1021/acs.inorgchem.2c04008
Inorg. Chem. XXXX, XXX, XXX−XXX

the type $Ph_2PCH_2CH_2P(CH_2CH_2CO_2Z)_2$ (Z = CO_2Me, CO_2Na), coordinate to Tc(V) and Re(V), to yield complexes of stoichiometry $[M(O)_2(diphos)_2]^+$ (M = ^{nat}Re, ^{99m}Tc). We further show that diphosphine-glucose bioconjugates can be prepared from acrylamide derivatives of glucose and these new diphosphine-glucose derivatives can be labeled with ^{99m}Tc and ^{188}Re in near-quantitative radiochemical yields. The resulting ^{99m}Tc radiotracers exhibit high stability in biological milieu and have favorable biodistribution properties, as exemplified by *in vivo* SPECT imaging of these novel ^{99m}Tc-tracers in mice.

RESULTS

Initial Re(V) Coordination Studies. Reaction of the previously reported hydrophosphination-derived ligand **L1** with $[ReI(O)_2(PPh_3)_2]$ yielded a mixture of geometric isomers of $[Re(O)_2(\mathbf{L1})_2]^+$ (**1c** and **1t**) with the *trans*-$Re(O)_2$ core and the unsymmetrical diphosphines coordinated *cis* or *trans* (Scheme 3).[30] The $^{31}P\{^1H\}$ NMR spectrum showed two multiplets centered at δ_P 8.6 and 9.0 ppm with a coordination shift $\Delta\delta$ of ca. 25 ppm for both isomers (Figure S1).

Scheme 3. (a) Synthesis of L2-Na_2/L2-H_2; (b) Preparation of $[M(O)_2(L1)_2]^+$ and $[M(O)_2(L2\text{-}H_2)_2]^+$ (M = ^{99m}Tc, ^{nat}Re)[a]

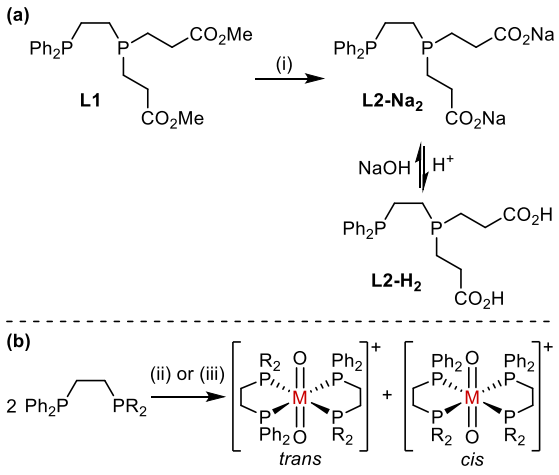

M	diphos	*trans*	*cis*	Yield / %
^{nat}Re	**L1**	**1t**	**1c**	85
^{nat}Re	**L2-H_2**	**2t**	**2c**	78
^{99m}Tc	**L1**	**3t**	**3c**	-
^{99m}Tc	**L2-H_2**	**4t**	**4c**	98

[a]Conditions: (i) NaOH (2 equiv), MeOH:H_2O (1:1), 79%; (ii) $[ReI(O)_2(PPh_3)_2]$, DCM; (iii) $[^{99m}TcO_4]^-$, Sn-containing kit. Yields given for combined *cis*/*trans*-$[M(O)_2(L)_2]^+$ and as radiochemical yields for ^{99m}Tc. Note that the overall charge on complexes of **L2-H_2** is dependent on pH since this will determine the degree of deprotonation of the carboxylic acid groups.

Crystals of *trans*-$[Re(O)_2(\mathbf{L1})_2]I$ (**1t**) suitable for X-ray crystallography were grown by slow diffusion of pentane into its methanol solution (Figure 1). The Re=O bond lengths (1.778(3) Å) and Re−P bond lengths (2.4651(16) and 2.4619(17) Å) are similar to the corresponding distances in the complex $[Re(O)_2(dmpe)_2]PF_6{\cdot}2H_2O$.[42]

Diester **L1** was hydrolyzed with NaOH in MeOH:H_2O (1:1) at ambient temperature and the product isolated as the moderately air-stable sodium salt **L2-Na_2** (Scheme 3(a)).

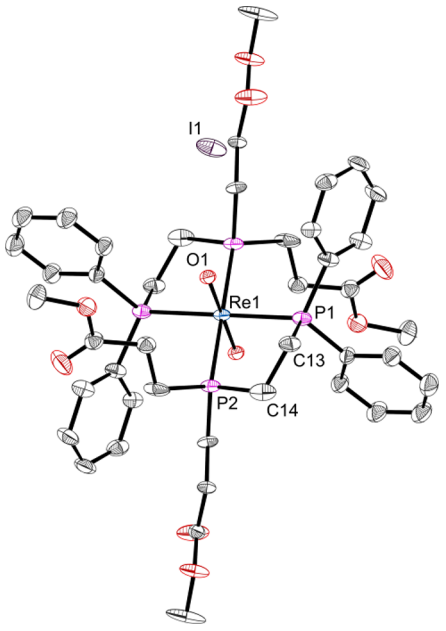

Figure 1. Molecular structure of *trans*-$[Re(O)_2(\mathbf{L1})_2]I$ from X-ray crystallographic analysis. Hydrogen atoms are omitted for clarity. Selected bond lengths (Å) and bond angles (deg): Re(1)−P(1) 2.4651(16), Re(1)−P(2) 2.4619(17), Re(1)−O(1) 1.778(3), O(1)−Re(1)−O(1) 180, P(1)−Re(1)−P(2) 80.29(5), P(1)−Re(1)−O(1) 96.60(12), P(2)−Re(1)−O(1) 90.49(13).

Treatment of $[ReI(O)_2(PPh_3)_2]$ with the derived dicarboxylate ligand **L2-Na_2** gave cationic Re(V) complexes as a mixture of *trans* and *cis* isomers **2t** and **2c** (Scheme 3(b)). The two geometric isomers were separated by reverse-phase HPLC (using an acidic mobile phase containing trifluoroacetic acid) and fully characterized; under these HPLC conditions, *trans*-$[Re(O)_2(\mathbf{L2\text{-}H_2})_2][CF_3CO_2]$ (**2t**) eluted first.

The signals observed by $^{31}P\{^1H\}$ NMR spectroscopy for **2t** and **2c**, were each simulated as AA′BB′ spin systems and the good agreement between the experimental and simulated spectra supports the assignment of the isomers (Figure 2).

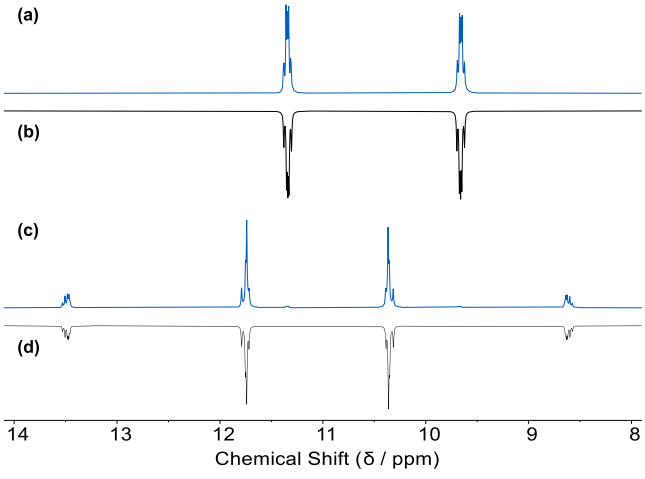

Figure 2. (a) Experimental and (b) simulated $^{31}P\{^1H\}$ NMR spectrum of *trans*-$[Re(O)_2(\mathbf{L2\text{-}H_2})_2]^+$ (**2t**); (c) experimental and (d) simulated $^{31}P\{^1H\}$ NMR spectrum of *cis*-$[Re(O)_2(\mathbf{L2\text{-}H_2})_2]^+$ (**2c**). See SI for the details of the simulations.

https://doi.org/10.1021/acs.inorgchem.2c04008
Inorg. Chem. XXXX, XXX, XXX−XXX

^{99m}Tc-Radiolabeling of Diester L1 and Dicarboxylate L2-Na$_2$. ^{99m}Tc-based radiopharmaceuticals are often formulated from an instant "kit" that contains all the required nonradioactive chemicals.[43] These kits enable routine, simple, one-step preparations of ^{99m}Tc-labeled radiotracers in hospital radiopharmacies, simply by addition of generator-produced $[^{99m}TcO_4]^-$ dissolved in saline solution to a kit vial, followed by incubation at ambient or elevated temperatures. The ratios of the components of the lyophilized kits produced in this work were based on *Myoview* kits and consisted of either **L1** or **L2-Na$_2$** diphosphine ligand, stannous chloride as reducing agent, sodium bicarbonate as buffer, and either sodium tartrate or sodium D-gluconate which coordinates to reduced ^{99m}Tc intermediates, to prevent their hydrolysis and formation of insoluble ^{99m}Tc-containing suspensions (see Table S1).

In an initial ^{99m}Tc-radiolabeling experiment, a solution of aqueous $[^{99m}TcO_4]^-$ was added to a lyophilized kit containing **L1**, and the mixture was heated at 60 °C for 30 min (Scheme 3(b)). Reverse-phase HPLC analysis indicated that numerous ^{99m}Tc-labeled species had formed in >90% radiochemical yield (see Figure S2); the complexity of the product mixture is attributed to the formation of hydrolyzed ester products as *cis* and *trans* isomers.

To obviate the difficulties of analyzing the mixture of reaction products formed from diester **L1**, ^{99m}Tc-radiolabeling studies were instead undertaken with dicarboxylate chelator, **L2-Na$_2$**. Aqueous $[^{99m}TcO_4]^-$ was added to the kit containing **L2-Na$_2$**, and the reaction mixture set aside at ambient temperature for 30 min. HPLC analysis revealed the formation of two major species, with retention times of 10 and 13 min, formed in 39% and 59% radiochemical yields, respectively (see Figure S3); these products are assigned to *trans*-$[^{99m}Tc(O)_2(\mathbf{L2\text{-}H_2})_2]^+$ (**3t**) and *cis*-$[^{99m}Tc(O)_2(\mathbf{L2\text{-}H_2})_2]^+$ (**3c**). A low intensity radioactive signal at 2 min (ca. 2% of detected ^{99m}Tc) is attributed to ^{99m}Tc intermediates or unreacted $[^{99m}TcO_4]^-$. The ^{99m}Tc radiolabeling experiment was repeated and spiked with $[^{99g}TcO_4]^-$ (^{99g}Tc, $t_{1/2} = 2 \times 10^5$ years) so that Tc complexes could be analyzed further. The ^{99g}Tc/^{99m}Tc-labeled products were collected and analyzed by negative ion MALDI MS and signals corresponding to $[M-2H]^-$ ($[C_{40}H_{48}O_{10}P_4{}^{99}Tc]^-$) were observed at m/z = 909.1, consistent with the assigned stoichiometry of these complexes, and indicating that the two ^{99}Tc-labeled species are isomeric.

Synthesis and ^{nat}Re(V) Coordination Chemistry of Diphosphine Glycoconjugates. Having established that simple, unsymmetrical diphosphines coordinate to ^{99m}Tc(V), we aimed to prepare more complex diphosphine bioconjugates, and selected two glucose derivatives to demonstrate the feasibility of applying a Pt(0)-catalyzed hydrophosphination reaction to derivatize diphosphines with biologically relevant molecules.

The glucose substrates **5** and **6** bearing an activated alkene at *C*1 and *C*2, respectively, were synthesized as shown in Scheme 4. Initially, **5** was synthesized via an azide derivative, as described in the SI, while the larger scale synthesis was achieved in two steps in 58% yield from acrylation and then acetylation of β-D-glucopyranosylammonium carbamate. Substrate **6** was synthesized in 3 steps and 46% overall yield from glucosamine hydrochloride (GlcNH·HCl) by installation of the β-OMe followed by acrylation.

The *C*1-conjugate **5** was subjected to the Pt(0)-catalyzed hydrophosphination conditions, using 2.5 mol % $[Pt(nbe)_3]$ (nbe = norbornene) and *i*-PrOH (20 equiv) as the protic additive, to give diphosphine glycoconjugate **L3** in 82% isolated yield (Scheme 5). It was found that *i*-PrOH was also a suitable protic additive in these reactions, and more convenient than *t*-BuOH which is a semisolid at room temperature. Hydrophosphination of the *C*2-conjugate **6** gave an unknown byproduct which was characterized by two doublet signals at δ_P +38.6 and −12.9 ppm ($^3J_{P,P}$ = 44.6 Hz) in the $^{31}P\{^1H\}$ NMR spectrum of the crude material (Figure S4). Increasing the catalyst loading to 5.0 mol % reduced the amount of byproduct and pure **L4** was isolated in 55% yield. Investigations into the identity of the unknown byproduct are ongoing. Acetate deprotection of the glucose motifs in both diphosphine glycoconjugates, **L3** and **L4**, using NaOMe gave ligands **L5** (74%) and **L6** (82%), respectively.

Scheme 4. Synthesis of Glucose Substrates 5 and 6 Bearing an Activated Alkene at *C*1 and *C*2, Respectively[a]

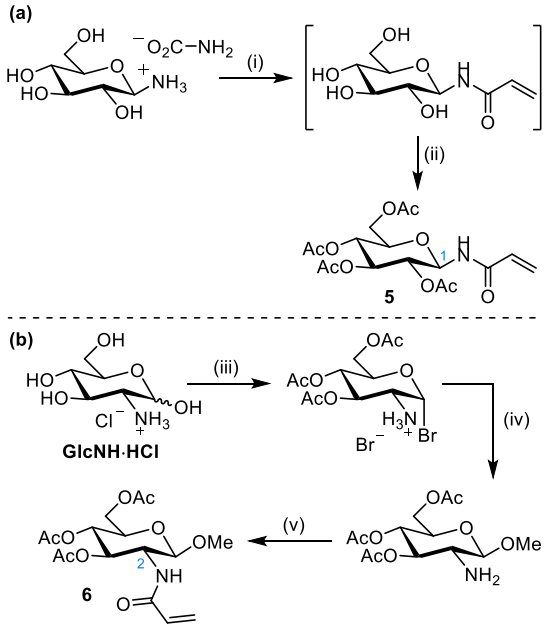

[a]Conditions: (i) Na_2CO_3 (5.7 equiv), MeOH:H_2O (1:1) then acryloyl chloride (3.2 equiv) in THF at 0 °C; (ii) Ac_2O, pyridine, 58% over two steps; (iii) acetyl bromide, 78%; (iv) MeOH, pyridine, 65%; (v) acryloyl chloride (1.2 equiv), NEt_3 (1.5 equiv), DCM, 91%.

The Pt(0)-catalyzed hydrophosphination of activated alkenes is a reliable reaction, and we have now found that this reaction takes place even in aqueous media. Thus, **L6** was made by Pt(0)-catalyzed hydrophosphination of the unprotected glucose acylamide precursor in 20% aqueous isopropanol (Scheme 5). Significantly, this aqueous chemistry opens up the possibility of using highly hydrophilic activated alkenes as substrates for hydrophosphination.

The diphosphine glycoconjugate ligands **L5** and **L6** were each reacted with $[ReI(O)_2(PPh_3)_2]$ (Scheme 6), furnishing *cis*- and *trans*-$[Re(O)_2(\mathbf{L})_2]^+$ (**7c**/**7t** and **8c**/**8t**) as expected. The *cis* and *trans* isomers of these complexes are distinguishable by $^{31}P\{^1H\}$ NMR spectroscopy based on the characteristic AA′BB′ patterns for each isomer, which are very similar to those observed for the analogous **L2-H$_2$** complexes (**2c** and **2t**, see Figure 2). The two geometric isomers of $[Re(O)_2(\mathbf{L5})_2]^+$ (**7c** and **7t**) were separated by reverse-phase HPLC and characterized separately (Figure S5). After 4 days in solution, isomerization of originally pure samples of **7c** and **7t** was detected by $^{31}P\{^1H\}$ NMR spectroscopy (Figures S6 and S7).

https://doi.org/10.1021/acs.inorgchem.2c04008
Inorg. Chem. XXXX, XXX, XXX−XXX

Scheme 5. Synthesis of Diphosphine Glycoconjugates via Pt(0)-Catalyzed Hydrophosphination[a]

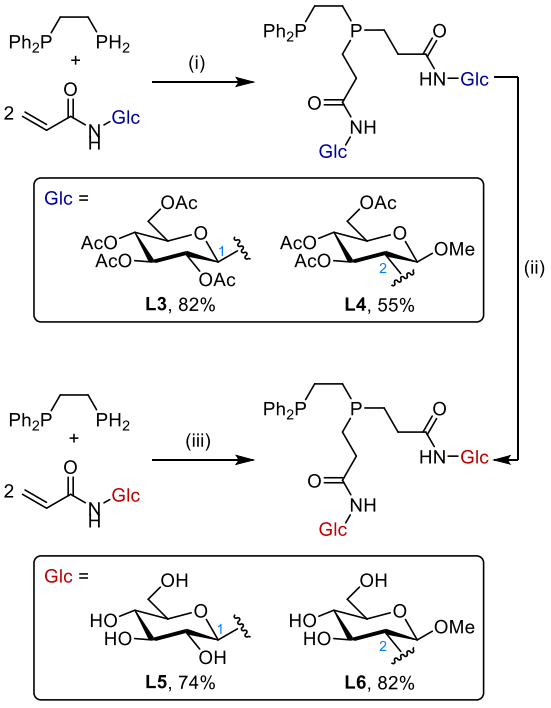

[a]Conditions: (i) 2.5% or 5.0% [Pt(nbe)$_3$], *i*-PrOH (20 equiv); (ii) NaOMe (0.2 mol %) in MeOH; (iii) 5.0% [Pt(nbe)$_3$] in 20% aqueous *i*-PrOH gave **L6** in 80% yield (determined by $^{31}P\{^1H\}$ NMR spectroscopy).

Scheme 6. Coordination and Radiolabeling of L5 and L6 to Form $[M(O)_2(L)_2]^+$, where M = ^{nat}Re, ^{188}Re, and ^{99m}Tc[a]

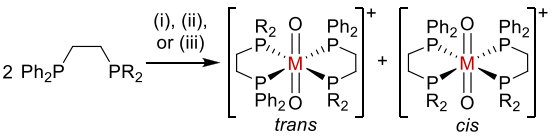

M	diphos	*trans*	*cis*	Yield / %
^{nat}Re / ^{188}Re	**L5**	**7t / 7t***	**7c / 7c***	98 / 97
^{nat}Re / ^{188}Re	**L6**	**8t / 8t***	**8c / 8c***	96 / 99
^{99m}Tc	**L5**	**9t**	**9c**	99
^{99m}Tc	**L6**	**10t**	**10c**	96

[a]Conditions: (i) [ReI(O)$_2$(PPh$_3$)$_2$], MeOH; (ii) $^{99m}TcO_4^-$, Sn-containing kit; (iii) $^{188}ReO_4^-$, $SnCl_2$, sodium citrate. Yields given for combined *cis*/*trans*-$[M(O)_2(L)_2]^+$ and as radiochemical yields for ^{99m}Tc and ^{188}Re. The asterisk in compound numbers (e.g., **7t***) denotes a ^{188}Re radiolabeled isotopologue.

After 20 days, there were no further spectroscopic changes in either of the samples indicating that equilibration was complete. At equilibrium, an approximately 1:1 mixture of **7c** and **7t** was observed indicating that the equilibrium constant $K \approx 1$. The kinetics of the *cis*/*trans* isomerization are slow enough to suggest that the individual isomers would retain their integrity on a clinical time scale.

^{99m}Tc and ^{188}Re Radiolabeling of Diphosphine Glycoconjugates L5 and L6. The new glycoconjugate **L5** was selected for more detailed radiochemical and biological evaluation, as it was thought that the fully unprotected glucose motif in **L5** would be more likely to retain glucose recognition when compared with **L6**, which is linked via *C*2 and contains a OMe group at the *C*1 position. Lyophilized mixtures of **L5**, stannous chloride, sodium gluconate, and sodium bicarbonate were prepared, providing prefabricated "kits", similar to those prepared for ^{99m}Tc-radiolabeling reactions with **L1** and **L2-Na$_2$** (see above). A saline solution containing generator-produced $[^{99m}TcO_4]^-$ (220−280 MBq) was added to a kit, and the mixture was then left to react at ambient temperature (20−25 °C) for 5 min. Radio-HPLC analysis of this mixture revealed formation of *trans*-$[^{99m}Tc(O)_2(\mathbf{L5})_2]^+$ (**9t**) (7.88 min) and *cis*-$[^{99m}Tc(O)_2(\mathbf{L5})_2]^+$ (**9c**) (12.51 min) in exceptionally high radiochemical yields of 70% and 29%, respectively, with <1% of ^{99m}Tc present as unreacted $[^{99m}TcO_4]^-$ or other ^{99m}Tc species (Figure 3a).

The radionuclide, ^{188}Re, is available from a ^{188}W/^{188}Re generator. Radioactive decay of parent ^{188}W ($t_{1/2}$ = 69 days) to

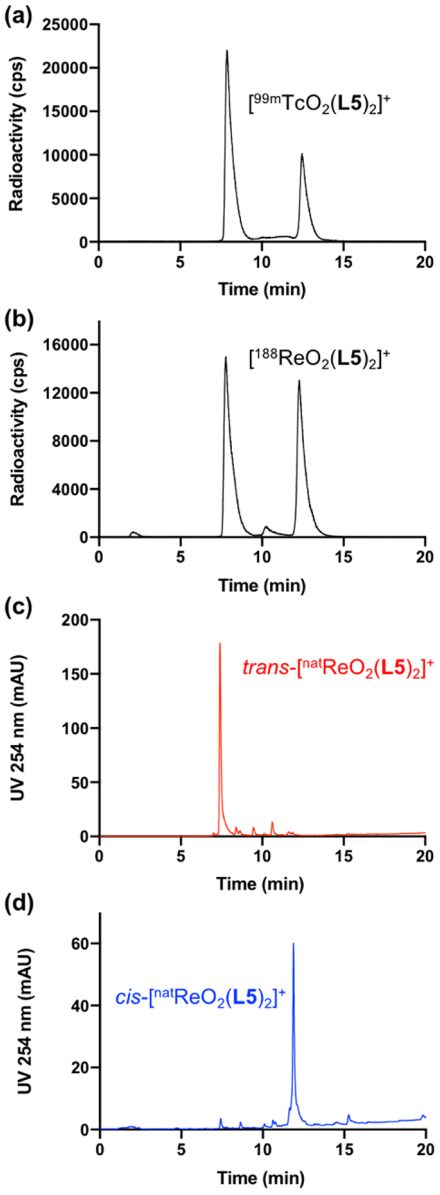

Figure 3. Analytical reverse-phase HPLC chromatograms of (a) $[^{99m}Tc(O)_2(\mathbf{L5})_2]^+$ (**9c** and **9t**); (b) $[^{188}Re(O)_2(\mathbf{L5})_2]^+$ (**7c*** and **7t***); (c) *trans*-$[^{188}Re(O)_2(\mathbf{L5})_2]^+$ (**7t**); (d) *cis*-$[^{188}Re(O)_2(\mathbf{L5})_2]^+$ (**7c**).

https://doi.org/10.1021/acs.inorgchem.2c04008
Inorg. Chem. XXXX, XXX, XXX−XXX

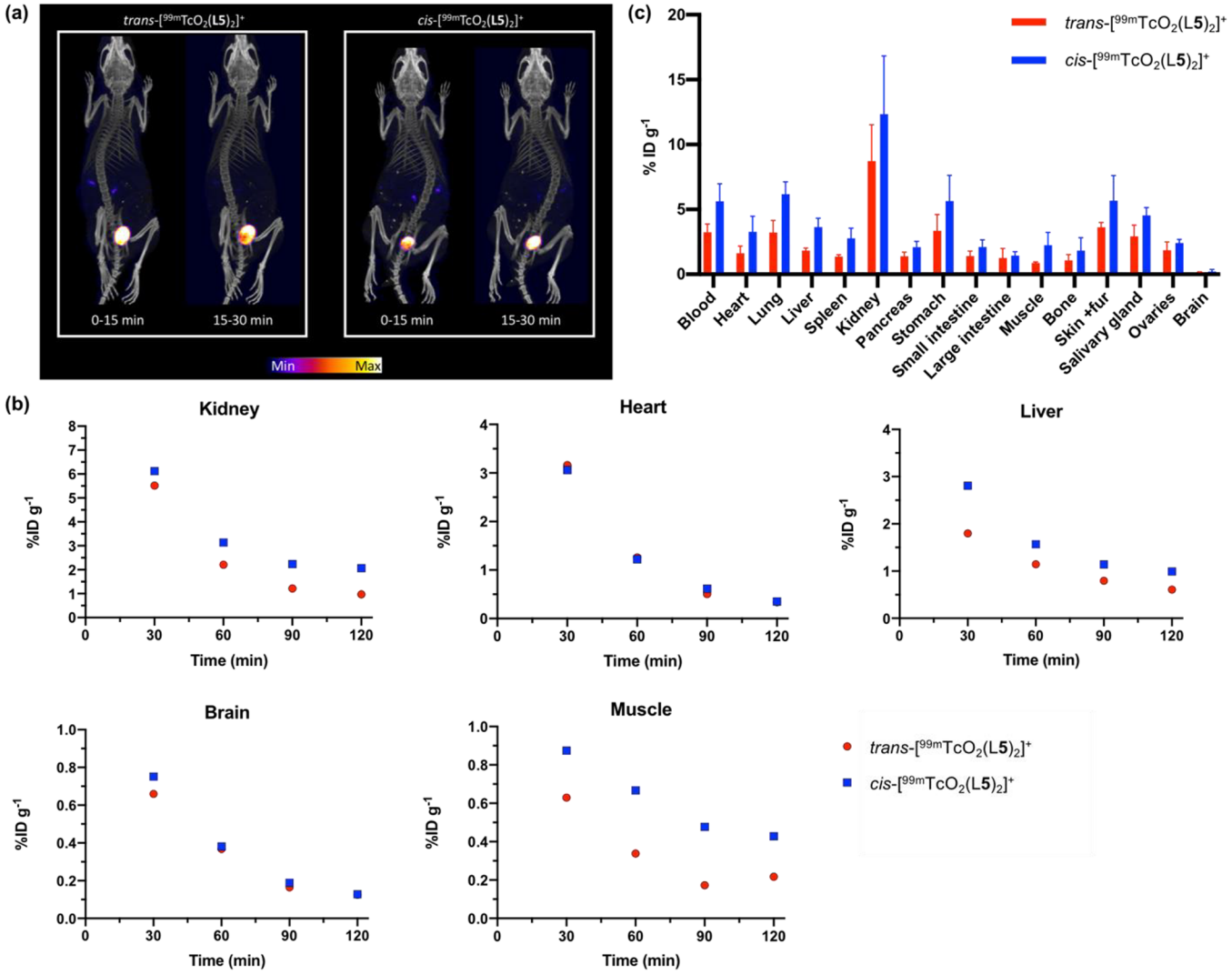

Figure 4. (a) SPECT/CT maximum intensity projections of healthy Balb/c mice administered and **9c** and **9t**; (b) SPECT image analysis of healthy Balb/c mice administered **9c** and **9t**. Regions of interest were selected on VivoQuant (inviCRO, LLC, Boston, USA), and percentage injected dose per milliliter (% ID/mL) were calculated for each of **9c** (n = 1) and **9t** (n = 1). (c) Biodistribution (30 min postinjection) of mice, administered either **9c** or **9t** intravenously (n = 4 per group).

^{188}Re enables a continuous source of ^{188}Re for 6−24 months (depending on user requirements). ^{188}Re is eluted from the generator by saline solution, in the form of $[^{188}ReO_4]^-$. To assess the ability of diphosphines to complex medically useful radioisotopes of Re, **L5** was radiolabeled with ^{188}Re. First, $[^{188}ReO_4]^-$ was reduced to a Re(V)-citrate precursor, by heating a saline solution of $[^{188}ReO_4]^-$ with stannous chloride at 90 °C in the presence of sodium citrate.[9,11] Diphosphine **L5** was then added to a solution containing the ^{188}Re(V)-citrate precursor, and the mixture heated at 90 °C for 30 min to yield *trans*-$[^{188}Re(O)_2(\mathbf{L5})_2]^+$ (**7t***) (7.80 min) and *cis*-$[^{188}Re(O)_2(\mathbf{L5})_2]^+$ (**7c***) (12.31 min) in 52% and 45% radiochemical yield, respectively (Figure 3b). The very similar retention times of ^{99m}Tc and ^{188}Re analogues are consistent with these complexes being isostructural. A third, unidentified species (10.57 min) was formed in 2% radiochemical yield.

The ^{188}Re radiolabeling could also be accomplished at ambient temperature, with a reaction time of only 5 min; under these conditions, lower radiochemical yields of 45% for **7t*** and 40% for **7c*** were obtained (Figure S8). At ambient temperature, unreacted $[^{188}ReO_4]^-$/^{188}Re(V)-citrate precursor accounted for 7% of ^{188}Re radioactive species and an unidentified species was also formed in 8% radiochemical yield.

To confirm the identity of these radiolabeled products, the analogous, naturally occurring Re complexes were also analyzed by HPLC: **7t** eluted at 7.41 min and **7c** eluted at 11.89 min (Figure 3c−d). These ^{nat}Re species exhibit similar chromatographic properties to the analogous radioactive ^{99m}Tc and ^{188}Re compounds. The small difference in retention times between ^{nat}Re and ^{188}Re isotopologues is an artifact of the configuration of the UV and radioactivity (scintillation) detectors in series.

The diphosphine-glucose conjugate, **L6**, was also radiolabeled with ^{99m}Tc and ^{188}Re, using the same radiosynthetic procedures. Diphosphine **L6** was similarly incorporated into a lyophilized kit mixture for radiolabeling with ^{99m}Tc to give $[^{99m}Tc(O)_2(\mathbf{L6})_2]^+$ (**10c** and **10t**); **L6** was added to solutions of ^{188}Re(V)-citrate for radiolabeling to give $[^{188}Re(O)_2(\mathbf{L6})_2]^+$ (**8c*** and **8t***). Similar to **L5**, the putative *cis* and *trans* isomers were formed in high radiochemical yields (>96% for ^{99m}Tc isomers, >99% for ^{188}Re isomers; Figure S9).

https://doi.org/10.1021/acs.inorgchem.2c04008
Inorg. Chem. XXXX, XXX, XXX−XXX

Stability of *cis*- and *trans*-[^{99m}Tc(O)$_2$(L5)$_2$]$^+$ (9c and 9t) in Serum. The stabilities of the new radiotracers, **9c** and **9t**, in serum were evaluated. First, each isomer was isolated from the radiolabeling reaction mixture which included their separation from unreacted **L5**. Then **9c** and **9t** were separately incubated in human serum. Radio-HPLC analysis indicated that both isomers were very stable in serum: for **9c**, 99.7% remained intact after 2 h, decreasing to 95.0% after 24 h; for **9t**, 98.6% of the complex remained intact after 2 h, decreasing to 93.4% after 24 h (Figure S10).

SPECT/CT and Biodistribution of *cis*- and *trans*-[^{99m}Tc(O)$_2$(L5)$_2$]$^+$ (9c and 9t) in Healthy Mice. SPECT/CT images were acquired using **9c** and **9t** (Figure 4a). Each isomer was separately injected intravenously to healthy Balb/c female mice (fasted for 12−14 h prior to tracer administration), followed by SPECT scanning for 2 h. Both **9c** and **9t** cleared circulation rapidly, predominantly via a renal pathway. For mice that had been administered **9c**, 60% of ^{99m}Tc activity was associated with the bladder/urine 30 min postinjection. Similarly, for mice that had been administered **9t**, image quantification showed that by 30 min postinjection, 60% of ^{99m}Tc activity was associated with the bladder/urine. In other measured organs and tissue (including liver, muscle, kidneys, heart/blood pool, and brain) the concentration of ^{99m}Tc activity for both isomers decreased from 30 min postinjection to 2 h postinjection (Figure 4b).

Biodistribution studies were also undertaken, in which healthy Balb/c female mice were administered radiotracer (Figure 4c). Mice were culled 30 min postinjection, and their organs harvested for *ex vivo* weighing and tissue counting for radioactivity. For measured organs, the highest ^{99m}Tc radioactivity concentration was observed in the kidneys, with 12.3 ± 4.5%ID g^{-1} for **9c**, and 8.7 ± 2.8%ID g^{-1} for **9t**, consistent with SPECT images showing high renal excretion. Relatively low levels of ^{99m}Tc radioactivity concentration (<7%ID g^{-1}) were observed for all other measured organs. Notably, for many measured organs, average ^{99m}Tc radioactivity concentration was higher for animals administered **9c**, compared with animals administered **9t**. This is possibly a result of slightly higher blood retention of **9c**: blood activity measured 5.6 ± 1.3%ID g^{-1} for **9c**, and 3.2 ± 0.6%ID g^{-1} for **9t**, 30 min postinjection.

Urine was also collected from these mice. Radio-HPLC analysis (Figure 5) of urine showed that both **9c** and **9t** were excreted intact, consistent with the high serum stability observed for both radiotracers.

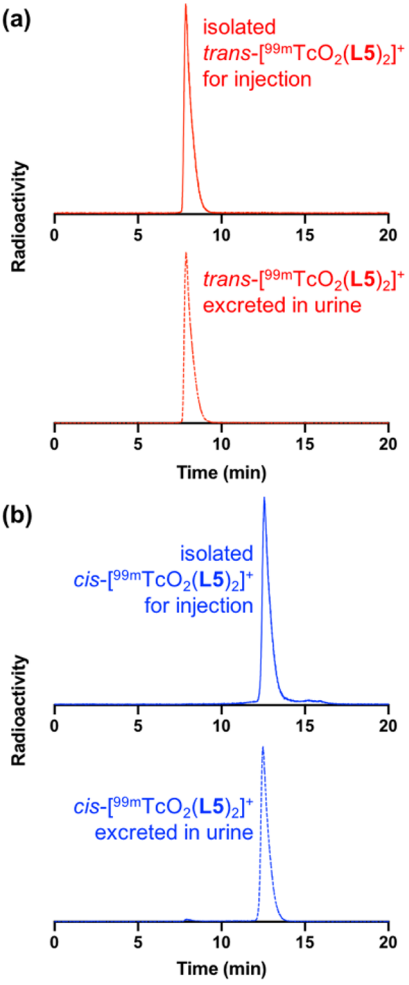

Figure 5. Radio-HPLC analysis of urine administered to mice intravenously administered either (a) **9t** or (b) **9c** shows that both radiotracers are excreted intact.

DISCUSSION

We have shown that Pt(0)-catalyzed hydrophosphination gives efficient access to biomolecule-functionalized diphosphines. The requisite acrylamide groups were straightforwardly introduced on two different glucose sites, namely, *C*1 or *C*2. Moreover, the ability to perform the reaction in *i*-PrOH (with 0−20% H_2O), with highly polar biomolecular derivatives to form diphosphine bioconjugates such as **L6**, expands the potential substrate scope to a large range of targeted, biologically active molecules. Additionally, it negates the need for common protecting groups, which are typically used to solubilize biomolecular precursors in nonpolar organic solvents to allow for synthetic derivatization. In turn, this removes the need for a deprotection reaction, in which conditions are often incompatible with newly introduced and sensitive phosphine groups. We envisage that other classes of biomolecules, including peptides and small molecules, could also be derivatized with acryl groups, allowing many compounds of biological relevance to be functionalized with a diphosphine.

Significantly, the resulting air-stable diphosphines are capable of quantitative radiolabeling of ^{99m}Tc(V) under mild reaction conditions. We undertook ^{99m}Tc radiolabeling of **L2-Na$_2$**, **L5**, and **L6** using lyophilized kits (containing phosphine ligand and reducing agent) and generator-produced [^{99m}TcO$_4$]$^-$, demonstrating the feasibility of using this diphosphine platform for rapid, one-step, kit-based ^{99m}Tc radiolabeling of receptor-targeted radiopharmaceuticals. The simple kit-based ^{99m}Tc radiolabeling methods described here are inspired by, and similar to, clinical protocols used for aseptic preparation of widely and routinely used perfusion agents. Notably, these radiolabeling methods contrast with the multistep, complicated procedures used for some newer, receptor-targeted ^{99m}Tc radiotracers currently being evaluated in clinical studies.[44] The ability to prepare ^{99m}Tc-labeled receptor-targeted radiotracers using a kit could increase access to receptor-targeted radiopharmaceuticals, and increase the utility and healthcare benefits of ^{99m}Tc and SPECT/γ-scintigraphy infrastructure.

Additionally, these new diphosphine bioconjugates chelate both ^{99m}Tc(V) and ^{188}Re(V)—the latter also in high

https://doi.org/10.1021/acs.inorgchem.2c04008
Inorg. Chem. XXXX, XXX, XXX−XXX

radiochemical yields (≥85%, even with only 5 min reaction at ambient temperature)—leading to the possibility of using this diphosphine bioconjugate platform for the development of a receptor-targeted, isostructural dual diagnostic/therapeutic pair (a "theranostic" agent) for molecular ^{99m}Tc SPECT imaging and ^{188}Re systemic radiotherapy.[7,45,46]

A further potential advantage of this platform is that multiple copies of a targeting motif can be introduced into a single molecule with relative ease. The hydrophosphination reaction here appends two copies of a targeting motif to each diphosphine; upon Tc(V) or Re(V) coordination, the number of copies increases to four per radiotracer molecule. Multimeric imaging agents, particularly those that incorporate peptides, have demonstrated increased *in vivo* accumulation at target tissue relative to their monomeric analogues, and are effective contrast agents.[47−49] There are a few examples in which ^{99m}Tc coordination by two equivalents of a chelator-peptide bioconjugate yields a radiotracer containing two copies of a targeting motif.[50−52] Our new diphosphine platform is eminently suited to developing molecular ^{99m}Tc/^{188}Re radiotracers containing multiple copies of a targeting group.

The new diphosphine bioconjugates yield radiotracers consisting of *cis* and *trans* geometric isomers. This is potentially a disadvantage, as prior to clinical application of any new radiotracer based on this platform, the isomers would likely require separate assessment to determine whether or not they are biologically equivalent to each other. However, we note that the ^{68}Ga-labeled prostate cancer radiotracer, ^{68}Ga-HBED-PSMA, consists of at least two distinct chemical species,[53,54] and yet despite this, the individual *in vivo* behavior of each of these species has not been assessed, and this has not prevented widespread and routine use of ^{68}Ga-HBED-PSMA.[55] Notably, the slow isomerization in solutions observed for *cis*- and *trans*-$[Re(O)_2(\mathbf{L5})_2]^+$ (**7c** and **7t**) was not observed for ^{99m}Tc analogues after 24 h in serum, nor in the excreted urine, suggesting that this isomerization appears to take place over a longer time scale than clinically relevant timeframes. Our initial *in vivo* characterization of each of *cis*-$[^{99m}Tc(O)_2(\mathbf{L5})_2]^+$ and *trans*-$[^{99m}Tc(O)_2(\mathbf{L5})_2]^+$ (**9c** and **9t**) shows that the two isomers have similar pharmacokinetic profiles to each other, with both exhibiting fast blood clearance via a renal pathway.

The development of a ^{99m}Tc-labeled, GLUT1-targeted radiotracer would enable γ-scintigraphy/SPECT imaging of metabolic status, providing a SPECT-equivalent radiopharmaceutical of the widely used PET diagnostic glucose analogue, [^{18}F]-FDG. There have been several previous attempts to label glucose or other carbohydrate derivatives with ^{99m}Tc for imaging of glucose uptake *in vivo*.[56] Some of these derivatives have demonstrated inhibitory activity of the hexokinase enzyme, which phosphorylates glucose in glucose metabolic pathways.[57−59] However, only a few of these ^{99m}Tc tracers demonstrate uptake in glucose-avid tissue.[59−62] Presumably this is due to lack of molecular recognition of modified/conjugated glucose moieties by GLUT1 and other GLUT receptors, which transport glucose into cells. Furthermore, it is possible that some of the ^{99m}Tc tracers that do show tumor accumulation are taken up via nonspecific mechanisms unrelated to GLUT1 expression. Although our new radiotracers contain four glucose units per molecule, SPECT/CT scanning in fasted mice showed no evidence of ^{99m}Tc retention in glucose-avid organs, such as the heart or brain, both of which demonstrate significant accumulation of ^{18}F in [^{18}F]-FDG PET scans.[63,64] Similar to the case of the great majority of ^{99m}Tc-labeled glucose derivatives, GLUT1 and other glucose transporters do not recognize the modified glucose moieties of **L5**.

Despite this absence of uptake of $[^{99m}Tc(O)_2(\mathbf{L5})_2]^+$ (**9c** and **9t**) in highly metabolic tissue, the high stability and rapid blood clearance of both **9c** and **9t**, and the lack of accumulation of ^{99m}Tc activity in healthy organs is auspicious. It suggests that other, more targeted radiotracers based on this platform will be similarly stable *in vivo* and have low off-target accumulation, and will hence provide high contrast SPECT/γ-scintigraphy images. In the case of any complementary ^{188}Re derivatives, the rapid clearance of these agents from healthy tissue would minimize radiation doses to healthy organs. While the four glucose units of $[^{99m}Tc(O)_2(\mathbf{L5})_2]^+$ no doubt contribute to the favorable clearance of $[^{99m}Tc(O)_2(\mathbf{L5})_2]^+$, it is plausible that other radiotracers based on this platform (for example, derivatives containing hydrophilic receptor-targeted peptides) will possess similarly favorable biodistribution properties. In this regard, we recently reported the RGD-conjugated diphosphine complexes of ^{nat}Re (**10c**/**10t**) and ^{99m}Tc (**11c**/**11t**) shown in Chart 2, where RGD is a cyclic peptide that targets $\alpha_v\beta_3$-integrin receptors. While complexes **10** and **11** were shown to target diseased tissue, the synthesis of the diphosphine has some limitations including the variation of the diphosphine structure. In contrast, it can readily be envisaged how RGD could be incorporated into a wide range of diphosphines by adaptation of the versatile hydrophosphination route reported here.

Chart 2. RDG-Conjugated Diphosphine Complexes

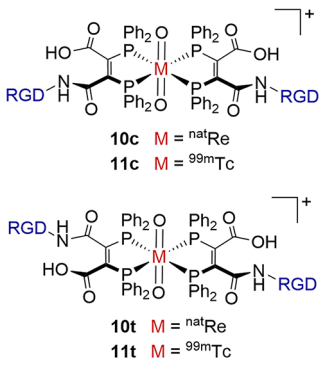

10c M = ^{nat}Re
11c M = ^{99m}Tc

10t M = ^{nat}Re
11t M = ^{99m}Tc

CONCLUSIONS

New chelator platforms that enable simple and efficient labeling of receptor-targeted biomolecules with radiometals have utility in nuclear medicine. We have demonstrated that diphosphines functionalized with glucose units can be efficiently prepared using Pt(0)-catalyzed hydrophosphinations of acrylamides. Notably, it has also been demonstrated that the hydrophosphinations of hydrophilic, unprotected glucose derivatives can be accomplished in aqueous media. The resulting diphosphine-glucose bioconjugates can be radiolabeled with both ^{99m}Tc and ^{188}Re in near-quantitative radiochemical yields. SPECT imaging studies in mice provide evidence that the new ^{99m}Tc radiotracers possess propitious pharmacokinetic properties, and the requisite high metabolic stability. Our new chemical technology therefore has significant potential for the future development of theranostic

https://doi.org/10.1021/acs.inorgchem.2c04008
Inorg. Chem. XXXX, XXX, XXX−XXX

pairs of chemically analogous diagnostic ^{99m}Tc-labeled radiotracers and radiotherapeutic ^{188}Re-labeled agents.

■ ASSOCIATED CONTENT

Supporting Information

The Supporting Information is available free of charge at https://pubs.acs.org/doi/10.1021/acs.inorgchem.2c04008.

Experimental procedures and characterization data, including radiolabeling procedures, selected NMR spectra, supplementary figures, and X-ray crystallographic tables (PDF)

Accession Codes

CCDC 2160396 contains the supplementary crystallographic data for this paper. These data can be obtained free of charge via www.ccdc.cam.ac.uk/data_request/cif, or by emailing data_request@ccdc.cam.ac.uk, or by contacting The Cambridge Crystallographic Data Centre, 12 Union Road, Cambridge CB2 1EZ, UK; fax: +44 1223 336033.

■ AUTHOR INFORMATION

Corresponding Authors

M. Carmen Galan − *School of Chemistry, University of Bristol, Bristol BS8 1TS, United Kingdom*; Email: m.c.galan@bristol.ac.uk

Michelle T. Ma − *School of Biomedical Engineering and Imaging Sciences, King's College London, London SE1 7EH, United Kingdom*; orcid.org/0000-0002-3349-7346; Email: michelle.ma@kcl.ac.uk

Paul G. Pringle − *School of Chemistry, University of Bristol, Bristol BS8 1TS, United Kingdom*; orcid.org/0000-0001-7250-4679; Email: paul.pringle@bristol.ac.uk

Authors

Rachel E. Nuttall − *School of Chemistry, University of Bristol, Bristol BS8 1TS, United Kingdom; School of Biomedical Engineering and Imaging Sciences, King's College London, London SE1 7EH, United Kingdom*; orcid.org/0000-0002-3945-3096

Truc Thuy Pham − *School of Biomedical Engineering and Imaging Sciences, King's College London, London SE1 7EH, United Kingdom*

Ailis C. Chadwick − *School of Chemistry, University of Bristol, Bristol BS8 1TS, United Kingdom*

Ingebjørg N. Hungnes − *School of Biomedical Engineering and Imaging Sciences, King's College London, London SE1 7EH, United Kingdom*

George Firth − *School of Biomedical Engineering and Imaging Sciences, King's College London, London SE1 7EH, United Kingdom*; orcid.org/0000-0003-1603-5067

Martin A. Heckenast − *School of Chemistry, University of Bristol, Bristol BS8 1TS, United Kingdom*

Hazel A. Sparkes − *School of Chemistry, University of Bristol, Bristol BS8 1TS, United Kingdom*

Complete contact information is available at: https://pubs.acs.org/10.1021/acs.inorgchem.2c04008

Author Contributions

The manuscript was written through contributions of all authors. All authors have given approval to the final version of the manuscript.

Notes

The authors declare no competing financial interest.

■ ACKNOWLEDGMENTS

This research was supported by a Cancer Research UK Career Establishment Award (C63178/A24959), the EPSRC programme for Next Generation Molecular Imaging and Therapy with Radionuclides (EP/S032789/1, "MITHRAS"), Rosetrees Trust (M685, M606), the Wellcome Multiuser Equipment Radioanalytical Facility funded by Wellcome Trust (212885/Z/18/Z), the Centre for Medical Engineering funded by the Wellcome Trust and the Engineering and Physical Sciences Research Council (EPSRC) (WT088641/Z/09/Z), the European Research Council grant number ERC−COG:648239, and the Bristol Chemical Synthesis Centre for Doctoral Training, funded by EPSRC (EP/L015366/1), and the University of Bristol, for a PhD studentship (to R.E.N.).We would like to thank Dr Paul J. Gates of the University of Bristol, UK for determining the mass spectra of the technetium complexes.

■ REFERENCES

(1) Rivas, C.; Jackson, J. A.; Hungnes, I. N.; Ma, M. T. Radioactive Metals in Imaging and Therapy in *Comprehensive Coordination Chemistry III*; Elsevier, 2021; Chapter 9.21.

(2) Jackson, J. A.; Hungnes, I. N.; Ma, M. T.; Rivas, C. Bioconjugates of Chelators with Peptides and Proteins in Nuclear Medicine: Historical Importance, Current Innovations, and Future Challenges. *Bioconjugate Chem.* **2020**, *31*, 483−491.

(3) Hofman, M. S.; Emmett, L.; Sandhu, S.; Iravani, A.; Joshua, A. M.; Goh, J. C.; Pattison, D. A.; Tan, T. H.; Kirkwood, I. D.; Ng, S.; Francis, R. J.; Gedye, C.; Rutherford, N. K.; Weickhardt, A.; Scott, A. M.; Lee, S.-T.; Kwan, E. M.; Azad, A. A.; Ramdave, S.; Redfern, A. D.; Macdonald, W.; Guminski, A.; Hsiao, E.; Chua, W.; Lin, P.; Zhang, A. Y.; McJannett, M. M.; Stockler, M. R.; Violet, J. A.; Williams, S. G.; Martin, A. J.; Davis, I. D. [^{177}Lu]Lu-PSMA-617 Versus Cabazitaxel in Patients with Metastatic Castration-Resistant Prostate Cancer (TheraP): A Randomised, Open-Label, Phase 2 Trial. *Lancet* **2021**, *397*, 797−804.

(4) Strosberg, J.; El-Haddad, G.; Wolin, E.; Hendifar, A.; Yao, J.; Chasen, B.; Mittra, E.; Kunz, P. L.; Kulke, M. H.; Jacene, H.; Bushnell, D.; O'Dorisio, T. M.; Baum, R. P.; Kulkarni, H. R.; Caplin, M.; Lebtahi, R.; Hobday, T.; Delpassand, E.; Van Cutsem, E.; Benson, A.; Srirajaskanthan, R.; Pavel, M.; Mora, J.; Berlin, J.; Grande, E.; Reed, N.; Seregni, E.; Öberg, K.; Lopera Sierra, M.; Santoro, P.; Thevenet, T.; Erion, J. L.; Rusziewski, P.; Kwekkeboom, D.; Krenning, E. Phase 3 Trial of ^{177}Lu-Dotatate for Midgut Neuroendocrine Tumors. *N. Engl. J. Med.* **2017**, *376*, 125−135.

(5) Treglia, G.; Castaldi, P.; Rindi, G.; Giordano, A.; Rufini, V. Diagnostic Performance of Gallium-68 Somatostatin Receptor PET and PET/CT in Patients with Thoracic and Gastroenteropancreatic Neuroendocrine Tumours: A Meta-Analysis. *Endocrine* **2012**, *42*, 80−87.

(6) Davies, L. H.; Kasten, B. B.; Benny, P. D.; Arrowsmith, R. L.; Ge, H.; Pascu, S. I.; Botchway, S. W.; Clegg, W.; Harrington, R. W.; Higham, L. J. Re and ^{99m}Tc Complexes of $BodP_3$ − Multi-Modality Imaging Probes. *Chem. Commun.* **2014**, *50*, 15503−15505.

(7) Cutler, C. S.; Hennkens, H. M.; Sisay, N.; Huclier-Markai, S.; Jurisson, S. S. Radiometals for Combined Imaging and Therapy. *Chem. Rev.* **2013**, *113*, 858−883.

(8) Kelly, J. D.; Forster, A. M.; Higley, B.; Archer, C. M.; Booker, F. S.; Canning, L. R.; Chiu, K. W.; Edwards, B.; Gill, H. K.; McPartlin, M.; Nagle, K. R.; Latham, I. A.; Pickett, R. D.; Storey, A. E.; Webbon, P. M. Technetium-99m-Tetrofosmin as a New Radiopharmaceutical for Myocardial Perfusion Imaging. *J. Nucl. Med.* **1993**, *34*, 222−227.

(9) Gali, H.; Hoffman, T. J.; Sieckman, G. L.; Owen, N. K.; Katti, K. V.; Volkert, W. A. Synthesis, Characterization, and Labeling with ^{99m}Tc/^{188}Re of Peptide Conjugates Containing a Dithia-Bisphosphine Chelating Agent. *Bioconjugate Chem.* **2001**, *12*, 354−363.

(10) Karra, S. R.; Schibli, R.; Gali, H.; Katti, K. V.; Hoffman, T. J.; Higginbotham, C.; Sieckman, G. L.; Volkert, W. A. ^{99m}Tc-Labeling

and in Vivo Studies of a Bombesin Analogue with a Novel Water-Soluble Dithiadiphosphine-Based Bifunctional Chelating Agent. *Bioconjugate Chem.* **1999**, *10*, 254−260.
(11) Kothari, K. K.; Gali, H.; Prabhu, K. R.; Pillarsetty, N.; Owen, N. K.; Katti, K. V.; Hoffman, T. J.; Volkert, W. A. Synthesis and Characterization of ^{99m}Tc- and ^{188}Re-Complexes with a Diamido-Dihydroxymethylenephosphine-Based Bifunctional Chelating Agent (N_2P_2-BFCA). *Nucl. Med. Biol.* **2002**, *29*, 83−89.
(12) Zeng, D.; Zeglis, B. M.; Lewis, J. S.; Anderson, C. J. The Growing Impact of Bioorthogonal Click Chemistry on the Development of Radiopharmaceuticals. *J. Nucl. Med.* **2013**, *54*, 829−832.
(13) Mindt, T. L.; Struthers, H.; Brans, L.; Anguelov, T.; Schweinsberg, C.; Maes, V.; Tourwé, D.; Schibli, R. 'Click to Chelate': Synthesis and Installation of Metal Chelates into Biomolecules in a Single Step. *J. Am. Chem. Soc.* **2006**, *128*, 15096−15097.
(14) Struthers, H.; Spingler, B.; Mindt, T. L.; Schibli, R. "Click-to-Chelate": Design and Incorporation of Triazole-Containing Metal-Chelating Systems into Biomolecules of Diagnostic and Therapeutic Interest. *Chem.—Eur. J.* **2008**, *14*, 6173−6183.
(15) Kluba, C. A.; Mindt, T. L. Click-to-Chelate: Development of Technetium and Rhenium-Tricarbonyl Labeled Radiopharmaceuticals. *Molecules* **2013**, *18*, 3206−3226.
(16) Zhao, Y.; Van Nguyen, H.; Male, L.; Craven, P.; Buckley, B. R.; Fossey, J. S. Phosphino-Triazole Ligands for Palladium-Catalyzed Cross-Coupling. *Organometallics* **2018**, *37*, 4224−4241.
(17) Laborde, C.; Wei, M. M.; Van Der Lee, A.; Deydier, E.; Daran, J. C.; Volle, J. N.; Poli, R.; Pirat, J. L.; Manoury, E.; Virieux, D. Double [3 + 2]-Dimerisation Cascade Synthesis of Bis(triazolyl)-bisphosphanes, a New Scaffold for Bidentate Bisphosphanes. *Dalton Trans.* **2015**, *44*, 12539−12545.
(18) Gusarova, N. K.; Arbusova, S. N.; Malysheva, S. F.; Khil'ko, M. Y.; Tatarinova, A. A.; Gorokhov, V. G.; Trofimov, B. A. Synthesis of Primary Phosphines from Phosphine and Arylethylenes. *Russ. Chem. Bull.* **1995**, *44*, 1535−1535.
(19) Wauters, I.; Debrouwer, W.; Stevens, C. V. Preparation of Phosphines Through C−P Bond Formation. *Beilstein J. Org. Chem.* **2014**, *10*, 1064−1096.
(20) Glueck, D. S. Catalytic Asymmetric Synthesis of P-Stereogenic Phosphines: Beyond Precious Metals. *Synlett* **2021**, *32*, 875−884.
(21) Glueck, D. S. Metal-Catalyzed P-C Bond Formation via P-H Oxidative Addition: Fundamentals and Recent Advances. *J. Org. Chem.* **2020**, *85*, 14276−14285.
(22) Delacroix, O.; Gaumont, A. C. Hydrophosphination of Unactivated Alkenes, Dienes and Alkynes: A Versatile and Valuable Approach for the Synthesis of Phosphines. *Curr. Org. Chem.* **2005**, *9*, 1851−1882.
(23) Moglie, Y.; González-Soria, M. J.; Martín-García, I.; Radivoy, G.; Alonso, F. Catalyst- and Solvent-Free Hydrophosphination and Multicomponent Hydrothiophosphination of Alkenes and Alkynes. *Green Chem.* **2016**, *18*, 4896−4907.
(24) Koshti, V.; Gaikwad, S.; Chikkali, S. H. Contemporary Avenues in Catalytic PH Bond Addition Reaction: A Case Study of Hydrophosphination. *Coord. Chem. Rev.* **2014**, *265*, 52−73.
(25) Liu, X. T.; Han, X. Y.; Wu, Y.; Sun, Y. Y.; Gao, L.; Huang, Z.; Zhang, Q. W. Ni-Catalyzed Asymmetric Hydrophosphination of Unactivated Alkynes. *J. Am. Chem. Soc.* **2021**, *143*, 11309−11316.
(26) Bange, C. A.; Waterman, R. Challenges in Catalytic Hydrophosphination. *Chem.—Eur. J.* **2016**, *22*, 12598−12605.
(27) Bissessar, D.; Egly, J.; Achard, T.; Steffanut, P.; Bellemin-Laponnaz, S. Catalyst-Free Hydrophosphination of Alkenes in Presence of 2-Methyltetrahydrofuran: A Green and Easy Access to a Wide Range of Tertiary Phosphines. *RSC Adv.* **2019**, *9*, 27250−27256.
(28) Espinal-Viguri, M.; King, A. K.; Lowe, J. P.; Mahon, M. F.; Webster, R. L. Hydrophosphination of Unactivated Alkenes and Alkynes Using Iron(II): Catalysis and Mechanistic Insight. *ACS Catal.* **2016**, *6*, 7892−7897.
(29) Sharpe, H. R.; Geer, A. M.; Lewis, W.; Blake, A. J.; Kays, D. L. Iron(II)-Catalyzed Hydrophosphination of Isocyanates. *Angew. Chem., Int. Ed.* **2017**, *56*, 4845−4848.
(30) Chadwick, A. C.; Heckenast, M. A.; Race, J. J.; Pringle, P. G.; Sparkes, H. A. Self-Replication of Chelating Diphosphines via Pt(0)-Catalyzed Hydrophosphination. *Organometallics* **2019**, *38*, 3871−3879 and references therein.
(31) Pringle, P. G.; Smith, M. B. Platinum(0)-Catalysed Hydrophosphination of Acrylonitrile. *J. Chem. Soc., Chem. Commun.* **1990**, 1701−1702.
(32) Costa, E.; Pringle, P. G.; Smith, M. B.; Worboys, K. Self-Replication of Tris(cyanoethyl)phosphine Catalysed by Platinum Group Metal Complexes. *J. Chem. Soc., Dalton Trans.* **1997**, 4277−4282.
(33) Costa, E.; Pringle, P. G.; Worboys, K. Chemoselective Platinum(0)-Catalysed Hydrophosphination of Ethyl Acrylate. *Chem. Commun.* **1998**, 49−50.
(34) Wicht, D. K.; Kourkine, I. V.; Kovacik, I.; Glueck, D. S.; Concolino, T. E.; Yap, G. P. A.; Incarvito, C. D.; Rheingold, A. L. Platinum-Catalyzed Acrylonitrile Hydrophosphination. P-C Bond Formation via Olefin Insertion into a Pt-P Bond. *Organometallics* **1999**, *18*, 5381−5394.
(35) Glueck, D. S. Catalytic Asymmetric Synthesis of Chiral Phosphanes. *Chem.—Eur. J.* **2008**, *14*, 7108−7117 and references therein.
(36) Sadow, A. D.; Haller, I.; Fadini, L.; Togni, A. Nickel(II)-Catalyzed Highly Enantioselective Hydrophosphination of Methacrylonitrile. *J. Am. Chem. Soc.* **2004**, *126*, 14704−14705.
(37) Scriban, C.; Kovacik, I.; Glueck, D. S. A Protic Additive Suppresses Formation of Byproducts in Platinum-Catalyzed Hydrophosphination of Activated Olefins. Evidence for P-C and C-C Bond Formation by Michael Addition. *Organometallics* **2005**, *24*, 4871−4874.
(38) Galan, M. C.; Benito-Alifonso, D.; Watt, G. M. Carbohydrate Chemistry in Drug Discovery. *Org. Biomol. Chem.* **2011**, *9*, 3598−3610.
(39) Calvaresi, E. C.; Hergenrother, P. J. Glucose Conjugation for the Specific Targeting and Treatment of Cancer. *Chem. Sci.* **2013**, *4*, 2319−2333.
(40) Ido, T.; Wan, C.-N.; Casella, V.; Fowler, J. S.; Wolf, A. P.; Reivich, M.; Kuhl, D. E. Labeled 2-Deoxy-D-Glucose Analogs. ^{18}F-Labeled 2-Deoxy-2-Fluoro-D-Glucose, 2-Deoxy-2-Fluoro-D-Mannose and ^{14}C-2-Deoxy-2-Fluoro-D-Glucose. *J. Label. Compd. Radiopharm.* **1978**, *14*, 175−183.
(41) Mamede, M.; Higashi, T.; Kitaichi, M.; Ishizu, K.; Ishimori, T.; Nakamoto, Y.; Yanagihara, K.; Li, M.; Tanaka, F.; Wada, H.; Manabe, T.; Saga, T. [^{18}F]FDG Uptake and PCNA, Glut-1, and Hexokinase-II Expressions in Cancers and Inflammatory Lesions of the Lung. *Neoplasia* **2005**, *7*, 369−379.
(42) Engelbrecht, H. P.; Cutler, C. S.; Jurisson, S. S.; den Drijver, L.; Roodt, A. Solid State Study on Rhenium Dimethylphosphinoethane Complexes: X-ray Crystal Structures of Trans-$[ReO_2(Dmpe)_2]PF_6 \cdot 2H_2O$, Trans-$[ReO(OH)(Dmpe)_2](CF_3SO_3)_2$, Trans-$[ReN(Cl)(Dmpe)_2]CF_3SO_3$ and Trans-$[ReCl_2(Dmpe)_2]ReO_4$. *Synth. React. Inorg. M.* **2005**, *35*, 83−99.
(43) Liu, S.; Chakraborty, S. ^{99m}Tc-Centered One-Pot Synthesis for Preparation of ^{99m}Tc Radiotracers. *Dalton Trans.* **2011**, *40*, 6077−6086.
(44) Hillier, S. M.; Maresca, K. P.; Lu, G.; Merkin, R. D.; Marquis, J. C.; Zimmerman, C. N.; Eckelman, W. C.; Joyal, J. L.; Babich, J. W. ^{99m}Tc-Labeled Small-Molecule Inhibitors of Prostate-Specific Membrane Antigen for Molecular Imaging of Prostate Cancer. *J. Nucl. Med.* **2013**, *54*, 1369−1376.
(45) Lepareur, N.; Lacœuille, F.; Bouvry, C.; Hindré, F.; Garcion, E.; Chérel, M.; Noiret, N.; Garin, E.; Knapp, F. F. R., Jr. Rhenium-188 Labeled Radiopharmaceuticals: Current Clinical Applications in Oncology and Promising Perspectives. *Front. Med.* **2019**, *6*, 132.
(46) Blower, P. J. A Nuclear Chocolate Box: The Periodic Table of Nuclear Medicine. *Dalton Trans.* **2015**, *44*, 4819−4844.

https://doi.org/10.1021/acs.inorgchem.2c04008
Inorg. Chem. XXXX, XXX, XXX−XXX

(47) Zia, N. A.; Cullinane, C.; Van Zuylekom, J. K.; Waldeck, K.; McInnes, L. E.; Buncic, G.; Haskali, M. B.; Roselt, P. D.; Hicks, R. J.; Donnelly, P. S. A Bivalent Inhibitor of Prostate Specific Membrane Antigen Radiolabeled with Copper-64 with High Tumor Uptake and Retention. *Angew. Chem.* **2019**, *131*, 15133−15136.
(48) Imberti, C.; Terry, S. Y. A.; Cullinane, C.; Clarke, F.; Cornish, G. H.; Ramakrishnan, N. K.; Roselt, P.; Cope, A. P.; Hicks, R. J.; Blower, P. J.; Ma, M. T. Enhancing PET Signal at Target Tissue in Vivo: Dendritic and Multimeric Tris(hydroxypyridinone) Conjugates for Molecular Imaging of $A_v\beta_3$ Integrin Expression with Gallium-68. *Bioconjugate Chem.* **2017**, *28*, 481−495.
(49) Li, Z.-B.; Cai, W.; Cao, Q.; Chen, K.; Wu, Z.; He, L.; Chen, X. ^{64}Cu-Labeled Tetrameric and Octameric RGD Peptides for Small-Animal PET of Tumor $\alpha_v\beta_3$ Integrin Expression. *J. Nucl. Med.* **2007**, *48*, 1162−1171.
(50) North, A. J.; Karas, J. A.; Ma, M. T.; Blower, P. J.; Ackermann, U.; White, J. M.; Donnelly, P. S. Rhenium and Technetium-Oxo Complexes with Thioamide Derivatives of Pyridylhydrazine Bifunctional Chelators Conjugated to the Tumour Targeting Peptides Octreotate and Cyclic-RGDfK. *Inorg. Chem.* **2017**, *56*, 9725−9741.
(51) Bordoloi, J. K.; Berry, D.; Khan, I. U.; Sunassee, K.; de Rosales, R. T. M.; Shanahan, C.; Blower, P. J. Technetium-99m and Rhenium-188 Complexes with One and Two Pendant Bisphosphonate Groups for Imaging Arterial Calcification. *Dalton Trans.* **2015**, *44*, 4963−4975.
(52) Hungnes, I. N.; Al-Salemee, F.; Gawne, P. J.; Eykyn, T.; Atkinson, R. A.; Terry, S. Y. A.; Clarke, F.; Blower, P. J.; Pringle, P. G.; Ma, M. T. One-Step, Kit-Based Radiopharmaceuticals for Molecular SPECT Imaging: A Versatile Diphosphine Chelator for ^{99m}Tc Radiolabelling of Peptides. *Dalton Trans.* **2021**, *50*, 16156−16165.
(53) Eder, M.; Neels, O.; Müller, M.; Bauder-Wüst, U.; Remde, Y.; Schäfer, M.; Hennrich, U.; Eisenhut, M.; Afshar-Oromieh, A.; Haberkorn, U.; Kopka, K. Novel Preclinical and Radiopharmaceutical Aspects of [^{68}Ga]Ga-PSMA-HBED-CC: A New PET Tracer for Imaging of Prostate Cancer. *Pharmaceuticals* **2014**, *7*, 779−796.
(54) Tsionou, M. I.; Knapp, C. E.; Foley, C. A.; Munteanu, C. R.; Cakebread, A.; Imberti, C.; Eykyn, T. R.; Young, J. D.; Paterson, B. M.; Blower, P. J.; Ma, M. T. Comparison of Macrocyclic and Acyclic Chelators for Gallium-68 Radiolabelling. *RSC Adv.* **2017**, *7*, 49586−49599.
(55) Hennrich, U.; Eder, M. [68Ga]Ga-PSMA-11: The First FDA-Approved ^{68}Ga-Radiopharmaceutical for PET Imaging of Prostate Cancer. *Pharmaceuticals* **2021**, *14*, 713.
(56) Bowen, M. L.; Orvig, C. 99m-Technetium Carbohydrate Conjugates as Potential Agents in Molecular Imaging. *Chem. Commun.* **2008**, 5077−5091.
(57) Schibli, R.; Dumas, C.; Petrig, J.; Spadola, L.; Scapozza, L.; Garcia-Garayoa, E.; Schubiger, P. A. Synthesis and In Vitro Characterization of Organometallic Rhenium and Technetium Glucose Complexes Against Glut 1 and Hexokinase. *Bioconjugate Chem.* **2005**, *16*, 105−112.
(58) Ferreira, C. L.; Ewart, C. B.; Bayly, S. R.; Patrick, B. O.; Steele, J.; Adam, M. J.; Orvig, C. Glucosamine Conjugates of Tricarbonylcyclopentadienyl Rhenium(I) and Technetium(I) Cores. *Inorg. Chem.* **2006**, *45*, 6979−6987.
(59) Yang, D. J.; Kim, C.-G.; Schechter, N. R.; Azhdarinia, A.; Yu, D.-F.; Oh, C.-S.; Bryant, J. L.; Won, J.-J.; Kim, E. E.; Podoloff, D. A. Imaging with ^{99m}Tc ECDG Targeted at the Multifunctional Glucose Transport System: Feasibility Study with Rodents. *Radiology* **2003**, *226*, 465−473.
(60) Zhang, X.; Ruan, Q.; Duan, X.; Gan, Q.; Song, X.; Fang, S.; Lin, X.; Du, J.; Zhang, J. Novel ^{99m}Tc-Labeled Glucose Derivative for Single Photon Emission Computed Tomography: A Promising Tumor Imaging Agent. *Mol. Pharmaceutics* **2018**, *15*, 3417−3424.
(61) Chen, Y.; Wen Huang, Z.; He, L.; Long Zheng, S.; Lian Li, J.; Lian Qin, D. Synthesis and Evaluation of a Technetium-99m-Labeled Diethylenetriaminepentaacetate−Deoxyglucose Complex ([^{99m}Tc]−DTPA−DG) as a Potential Imaging Modality for Tumors. *Appl. Radiat. Isot.* **2006**, *64*, 342−347.
(62) Chen, Y.; Xiong, Q.; Yang, X.; Huang, Z.; Zhao, Y.; He, L. Noninvasive Scintigraphic Detection of Tumor with ^{99m}Tc-DTPA-Deoxyglucose: An Experimental Study. *Cancer Biother. Radiopharm.* **2007**, *22*, 403−405.
(63) Toyama, H.; Ichise, M.; Liow, J.-S.; Modell, K. J.; Vines, D. C.; Esaki, T.; Cook, M.; Seidel, J.; Sokoloff, L.; Green, M. V.; Innis, R. B. Absolute Quantification of Regional Cerebral Glucose Utilization in Mice by ^{18}F-FDG Small Animal PET Scanning and 2-^{14}C-DG Autoradiography. *J. Nucl. Med.* **2004**, *45*, 1398−1405.
(64) Fueger, B. J.; Czernin, J.; Hildebrandt, I.; Tran, C.; Halpern, B. S.; Stout, D.; Phelps, M. E.; Weber, W. A. Impact of Animal Handling on the Results of ^{18}F-FDG PET Studies in Mice. *J. Nucl. Med.* **2006**, *47*, 999−1006.

https://doi.org/10.1021/acs.inorgchem.2c04008
Inorg. Chem. XXXX, XXX, XXX−XXX